文章编号: 1001－2060(2007)06－0661－04

大型热力发电机组能耗参数的统计分析与应用

李利平[1], 张春发[2], 牛玉广[1], 王惠杰[2]
(1. 华北电力大学 自动化学院, 河北 保定 071003; 2. 华北电力大学 能源与动力工程学院, 河北 保定 071003)

摘　要: 基于机组长期运行数据和在线性能计算数据, 统计分析了机组的实际性能特性, 提出与过程热力特性及热力试验标准相一致的机组性能稳定态判别准则。由筛选出的满足稳定态准则的数据统计分析分别得出了机组在不同的外界边界条件和不同运行参数下以及同一运行工况内在线性能计算模型输出的不确定度范围, 为基于模型的优化决策调整和诊断提供参考。统计得出的热力机组煤耗量特性曲线反映的是机组在实际运行条件下的真实特性, 并以厂内负荷分配方案为例, 验证了针对性经济运行措施的有效性。

关　键　词: 热力机组; 在线性能计算; 统计特性; 不确定度; 负荷分配

中图分类号: TK212　　文献标识码: A

引　言

实时数据库系统在电力企业的安装应用为机组性能在线计算系统提供了可靠的数据基础, 拥有长期的、完整的机组原始运行数据及性能数据成为可能。目前, 在热力机组性能评价与诊断方面的研究主要是围绕性能分析的热力学模型方法以及在线系统的设计实施等[1~2]。从数据分析角度研究的报道还相对较少, 文献[3]对测量数据进行了检测或校验, 文献[4]进行了数据关联分析。本文以机组在线性能系统长期运行的结果数据和 DCS 系统历史数据为基础, 进行适当的数据筛选, 从数据统计分析的角度揭示出机组性能的基本特性及在线性能计算模型的可靠性, 为机组运行决策提供参考, 同时也为不确定性相关方法的应用研究打下基础。

1　热力机组在线性能计算模型

大型热力机组一般配套有较完善的一次测量系统, 为基于热力学状态参数的系统性能计算创造了条件。根据热力系统的拓扑结构建立与系统结构一一对应的系统状态矩阵方程[5], 并以其为核心来计算系统的能耗率。图 1 为典型中间再热机组系统简化示意图, 其对应的系统状态矩阵方程为:

$$\begin{bmatrix} q_1 & & \\ \gamma_2 & q_2 & \cdots \\ \cdots & \cdots & \cdots \end{bmatrix} \begin{bmatrix} \sum D_1 \\ \sum D_2 \\ \cdots \end{bmatrix} + \begin{bmatrix} \sum q_{f1} \\ \sum q_{f2} \\ \cdots \end{bmatrix} = \begin{bmatrix} \tau_1 \sum D_{fw1} \\ \tau_2 \sum D_{fw2} \\ \cdots \end{bmatrix} \quad (1)$$

式中: q_i—单位质量抽汽在 i 加热单元的放热量, kJ; γ_i—单位质量疏水在 i 加热单元的放热量, kJ; τ_i—单位质量给水在 i 加热单元的焓增, kJ; $\sum D_i$—流经 i 加热单元抽汽侧(抽汽管道和疏水管路)的等效抽汽总量, kg/s; $\sum q_{fi}$—进出 i 加热单元的辅助等效热量, kJ; $\sum D_{fwi}$—流经 i 加热单元的等效给水量, kg/s。

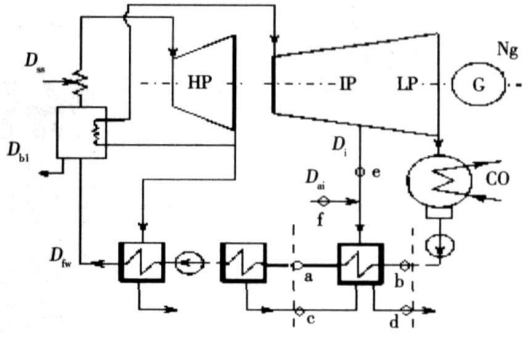

图 1　机组热力系统示意图

等效量的计算将根据具体加热器单元形式和辅助汽水流入(出)点所作的约定进行[5]。

将锅炉侧和汽轮机系统分别看作一个开口系, 由质量能量守恒可以得到系统的功率输出式(2)和吸热量式(3), 式中符号说明可参见文献[5]:

$$N = D_0(h_0 + \sigma - h_c) - [\boldsymbol{D}_i]^{\mathrm{T}}[\boldsymbol{h}_i^{\sigma}] - [\boldsymbol{D}_{\mathrm{X}i}]^{\mathrm{T}}[\boldsymbol{h}_i^{\sigma}] \quad (2)$$

$$Q = D_0(h_0 + \sigma - h_{fw}) - [\boldsymbol{D}_i]^{\mathrm{T}}_{\mathrm{H}}[\sigma] - [\boldsymbol{D}_{\mathrm{X}i}]^{\mathrm{T}}_{\mathrm{H}}[\sigma] +$$

收稿日期: 2007－01－10;　修订日期: 2007－08－15
基金项目: 国家自然科学基金资助项目(50576022)
作者简介: 李利平(1971－), 男, 陕西榆林人, 华北电力大学博士研究生;

$$D_{bl}(h_{bl}-h_{fw})+D_1(h_1-h_{fw})+D_{ss}(h_{fw}-h_{ss})+D_{rs}(h_{rh}-h_{rs}) \quad (3)$$

式(1)经过整理写成式(4):

$$[\boldsymbol{A}][\boldsymbol{D}_i]+[\boldsymbol{Q}_{fi}]=D_0[\tau_i] \quad (4)$$

则抽汽向量计算式为:

$$[\boldsymbol{D}_i]=[\boldsymbol{A}]^{-1}[D_0[\tau_i]-[\boldsymbol{Q}_{fi}]] \quad (5)$$

由式(5)计算出汽轮机各级抽汽量,一并代入其它相关状态参数到式(2)、式(3),即可得到汽轮机效率,再由相关参数计算获得锅炉效率等[6],即可得到机组的标准煤耗率。

2 基于历史数据的能耗率统计分析

以系统状态方程为核心的能耗率计算本质上是基于系统状态参数的热力计算。造成在线计算结果不确定性的主要因素为:(1) 现场测量仪表的精度、测量通道干扰;(2) 复杂热物理系统在多边界条件下的固有内在不确定性;(3) 热力学稳定态假设,也就是在当前工程领域所采用的基于系统状态参数的各种计算方法都是假定计算时刻系统处于稳定态。因此,当系统处于动态过程时采用该模型计算所得的性能数据并不代表系统性能的真实情况。

2.1 数据筛选原则

机组长期参与调峰运行,实时数据库中存在大量的机组升降负荷阶段的动态数据和其它不可用数据。数据筛选的基本思想是以机组热力试验中的电厂性能试验方案为参照标准,即保持系统不隔离,全部采用机组在线仪表的一次测量数据;ASME 标准要求系统的稳定期为 2 h[7],试验时间为 1 ~2 h,其目的是保证所有系统状态参量都进入试验要求的稳定范围内。通过对原始数据浏览,从热力学稳定态的角度看,闭式循环水入口温度是负荷调整后系统中过渡时间最长的状态量。当循环水入口温度保持稳定时,其它状态变量都已达到了稳定性要求。因此循环水入口温度的稳定才是热力学意义上的稳定工况,本文后面的统计分析都是基于热力学稳定工况数据。

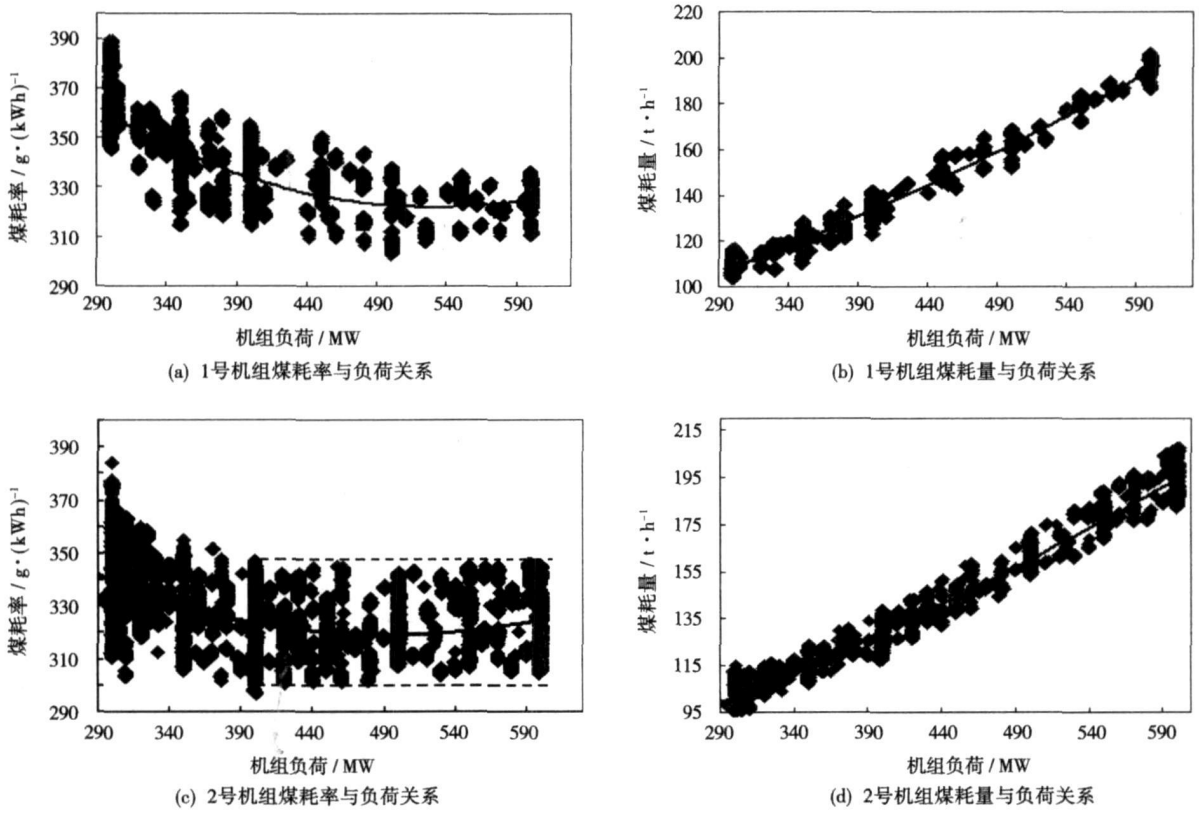

(a) 1号机组煤耗率与负荷关系 (b) 1号机组煤耗量与负荷关系

(c) 2号机组煤耗率与负荷关系 (d) 2号机组煤耗量与负荷关系

(a)、(b)由 1 号机组近 8 个月的原始数据中满足稳定条件的 278 个工况,以 1 min 为采样周期获得的 16 680 个数据点绘制

(c)、(d)由 2 号机组近 12 个月的原始数据中满足稳定条件的 322 个工况,以 1 min 为采样周期获得的 19 320 个数据点绘制

图 2 煤耗率及煤耗量与负荷间的关系

在原始数据中搜索满足热力学稳定工况数据的条件可表述为满足下列 3 个条件:

$$\begin{cases} t_{inv} \geqslant h_0 \\ |N_{max} - N_{min}| < \Delta_N \\ |TW_{max} - TW_{min}| < \Delta_{TW} \end{cases}$$

其中: t_{inv}—稳定工况的持续时间; h_0——一般可取 1 h 或以上; Δ_N、Δ_{TW}—机组负荷和循环水入口温度在该工况持续时间内保持在一定的范围内, 如取测量随机误差的标准差的 2 倍或其它适当数值。图 2(a)、(c)是由某厂两台 600 MW 机组近一年的数据筛选后得到的机组煤耗率与负荷的统计关系, (b)和(d)图为其对应的煤耗量与负荷的关系(常用于负荷分配)。

2.2　在线能耗率的不确定度范围

图 2 中的每一个点簇实际上就是一个稳定运行工况。结合其它参数的进一步分析得到如下统计结果:

(1) 影响热力机组性能最关键的两个边界条件是负荷和循环水入口温度, 其中从 100% 负荷到 50% 负荷范围内由于负荷引起的煤耗率变化范围约为 30 ~ 40 g/(kWh)。在一定负荷下, 循环水入口温度与煤耗率接近为线性关系, 温度每升高 1 ℃, 煤耗率增加约 1.3 ~ 1.5 g/(kWh)。

(2) 在同一负荷和循环水温度下, 由于运行方式、运行人员的偏好等不确定因素造成的煤耗率波动范围约为 20 g/(kWh)。

(3) 在同一个稳定工况内, 煤耗率的变化范围约为 2%, 也就是对于 600 MW 机组, 在线性能计算模型的不确定度范围约为 5 ~ 6 g/(kWh)。

2.3　统计分析结果讨论

统计分析结果得出的是系统在大量复杂边界条件组合情况下的一般特性。经验证, 图 2 所揭示的机组性能特性与机组的考核试验结果十分吻合。数据筛选环节已经排除了系统动态的影响。机组能耗率的不确定是由过程设备和测量仪表组成广义热物理系统在复杂边界条件和不同运行参数下内在本质不确定性的一种表现。基于实时数据的在线模型诊断结果反映的是包含设备安装、性能劣化、运行偏离、测量误差等因素在内的综合影响。虽然依赖于热力学模型的在线性能分析与诊断方法在电厂的运行监视、诊断分析等方面具有不可或缺的功能, 但在进一步缩小不确定度范围, 提高诊断决策能力方面还需从系统的不确定性本质出发结合相关理论方法研究。

3　几种负荷分配方法的经济性比较

由数据统计得到的机组能耗率分布特性更能直观地反映每一台机组的自身特性。下面以负荷分配为例说明统计分析结果的实用性。

3.1　最大效率法分配

通常机组负荷分配是根据每台机组煤耗量与负荷的关系曲线进行的, 如图 2(b)和(d)所示。由图可见, 煤耗量与负荷的关系曲线并不是很直观地反映机组的性能特性, 但由其对应的煤耗率曲线(a)和(c)可以看出, 1 号机的真实最低煤耗工况点为 500 MW 左右。2 号机的最低煤耗点为 400 MW 左右, 而且在 400 ~ 600 MW 之间煤耗率随负荷几乎不变, 具有良好的可调度性。为此, 采用最朴素的优化调度思想, 即最大效率法, 就是让每个机组都运行在最大效率点。在 900 ~ 1 100 MW 负荷段, 1 号机组固定负荷 500 MW, 2 号机组在 400 ~ 600 MW 调峰运行。

3.2　二次规划法分配

二次规划属于简单的约束非线性规划问题, 即目标函数为二次函数, 约束为线性函数。其一般形式为:

$$\begin{aligned} &\min f(x) = \frac{1}{2} x^{\mathrm{T}} G x + c^{\mathrm{T}} x \\ &s.t \quad Ax \leqslant b \\ &\qquad \hat{A}x = \hat{b} \\ &\qquad LB \leqslant x \geqslant UB \end{aligned}$$

式中: G—n 阶对称矩阵; A —$m \times n$ 阶矩阵; $\hat{A}$ —$t \times n$阶矩阵; LB、UB —x 的上下界。由图 2 中数据回归可得两机组的特性曲线:

$$F(P_1) = 0.000\ 169P_1^2 + 0.136P_1 + 52.03$$

$$F(P_2) = 0.000\ 176P_2^2 + 0.151P_2 + 41.01$$

则负荷分配优化目标为:

$$\begin{aligned} &\min B(P) = F(P_1) + F(P_2) \\ &s.t \quad P_1 + P_2 \leqslant 1200 \\ &\qquad P_1 + P_2 = P_{obj} \\ &\qquad 300 \leqslant P_1 \leqslant 600 \\ &\qquad 300 \leqslant P_2 \leqslant 600 \end{aligned}$$

式中: B—为总煤耗量; P_1、P_2、P_{obj}—单台机组的负荷值及当前总分配目标值。单台机组的调峰范围为 300 ~ 600 MW。本文采用 Matlab 优化工具箱中的 Quadprog 函数进行优化计算。

3.3　经济效益估算

3 种负荷分配方案下对应的煤耗量如表 1 所

示。可见,采用最大效率法在可调范围内分配负荷时,较之平均分配法可平均降低煤耗量 1.0 t/h 左右,若考虑两台机组均变动负荷时动态过程造成的额外煤耗量[8],这个差值可能还会更大。代入煤耗量差 1.0 t/h,10.0 h/天,300 天/年,500 元/t 计算得,每年可节约燃料费约 150 万元。由此可见基于更准确的机组特性的调度方案经济效益是很可观的。

表 1 两台机组在不同负荷分配方案下煤耗量比较 (t/h)

负荷点/MW	最大效率法	平均分配法[1]	二次规划法
800	—	262.8	262.4
900	289.3	291.7	291.4
950	305.4	306.9	306.5
1 000	321.5	322.4	322.1
1 050	337.6	338.4	338.0
1 100	353.7	354.8	354.4
1 200	388.9	388.9	388.9

注:1—该厂目前采用的负荷调度方法。

4 结 语

以机组热力过程特性及热力试验标准为指导,确立机组性能稳定态的判别标准,对机组大量原始运行数据进行筛选。由筛选出的有效数据进行统计分析,得出了机组在线性能模型计算结果在系统主要边界条件(负荷、循环水入口温度)下的不确定度范围;在相似外界边界条件,由于运行调整等引起的计算结果不确定度范围以及在同一边界条件下,由于测量不确定性等引起的计算结果不确定度范围。逐层深入,统计分析揭示出了不确定性是复杂热物理系统模型固有本质。不确定性相关理论方法应用是进一步提高模型决策可靠性的必然途径。由数据分析得到的机组特有的性能特性可为机组经济运行提供参考,本文以厂级负荷分配方案为例,比较了不同方案的经济性,为电力企业从多层面节能降耗提供一种有效思路。

参考文献:

[1] 李 勇,曹丽华,林文彬. 等效热降法的改进计算方法[J]. 中国电机工程学报,2004,26(12):36—40.

[2] 梁艳明,孙立明,贺晋卫. 火电厂 SIS 中在线性能计算与分析的应用[J]. 中国电力,2005,38(1):65—68.

[3] 刘福国,王学同. 基于系统测量冗余的电厂异常运行数据检测与校正[J]. 中国电机工程学报,2003,23(7):36—40.

[4] 王培红,陈 强,董益华,等. 数据挖掘及其在电厂 SIS 中的应用. 电力系统及其自动化,2004,28(4):76—79.

[5] 张春发. 现行电力系统热经济状态方程[J]. 工程热物理学报,2001,22(6):665—667.

[6] 范从振. 锅炉原理[M]. 北京:水利电力出版社,1986.

[7] 刘 凯. 汽轮机试验[M]. 北京:中国电力出版社,2005.

[8] YOSHIKAWA M. On-line economic load dispatch based on fuel cost dynamics[J]. IEEE Trans Power System,1997,12(1):315—320.

(编辑 柴 舒)

改造技术

利用计算空气动力学来改进汽轮机通流部分的设计

《Теплоэнергетика》2007 年 4 月号提供了在 T—100—12.8 型汽轮机高压缸现代化改造时利用反动式叶片装置对通流部分部件进行空气动力学修整的结果。

根据程序 SINF 完成了可压缩工质粘性紊流流动的数值模拟,确定被修整部件合理的形状。

得到了调节级室子午面轮廓的形状,保证最小的能量损失和可接受的流动径向不均匀性。说明了在小流入角下导向叶片应用流线形叶型的理由。

尽管在设计时对外形尺寸有严格的限制,在 T—100 型汽轮机高压缸通流部分改造时,应用数值模拟方法建立了具有良好气动力特性的调节级室的形状和第二级导向叶片的叶型。

通过验算,证明了高压缸通流部分部件形状选择的合理性。

(吉桂明 供稿)

不同密度煤粉的矿物质分布与燃烧特性研究＝**A Study of the Mineral Distribution and Combustion Characteristics of Pulverized Coal of Different Densities**[刊, 汉] / CAI You-min, YAO Hong, LIU Xiao-wei, et al (National Key Laboratory on Coal Combustion, Huazhong University of Science and Technology, Wuhan, China, Post Code: 430074) // Journal of Engineering for Thermal Energy & Power. — 2007, 22(6). — 651 ~ 655

Through the use of a heavy-liquid floatation, a kind of bituminous coal can be divided into three density sections, i.e. high (> 2.0 g/cm^3), medium (1.4 ~ 2.0 g/cm^3) and low (< 1.4 g/cm^3). By utilizing SEM, XRD and XRF etc. analytic methods, a study was conducted of mineral distribution, mineral composition, particle diameter, ash constituents, industrial and elementary analysis and combustion characteristics of raw coal of different densities. The results show that with an increase in density of the raw coal, the industrial analysis indicates an increase of ash content in coal, a decrease of volatile and fixed carbon content. The elementary analysis also indicates a decrease of organic carbon, element hydrogen and nitrogen content. Low-density pulverized coal contains a small amount of internal mineral matter while medium and high-density pulverized coal contain an abundance of mineral matter. What differs is that the former contains a great deal of internal mineral matter, but in the latter a large quantity of external mineral matter predominates. The particle diameter distribution of the raw coal of three densities is almost identical. However, the particle diameter distribution of the mineral matter contained in the raw coal in question is very different. With an increase of the density of raw coal, the particle diameter of mineral matter contained in it will increase significantly. The thermogravimetric curves of the raw coal of three densities indicate that the low-density pulverized coal assumes a most intense combustion and the weight loss and heat release become ever weaker with an increase of density. **Key words**: coal, density, mineral matter, granularity, thermogravimetry

螺旋通道内受限外流传热和阻力特性的数值模拟＝**Numerical Simulation of Heat Transfer and Resistance Characteristics of the Restricted Outgoing Flow in a Spiral Channel**[刊, 汉] / LEI Yong-gang, CHU Pan, HE Ya-ling, et al (National Key Laboratory on Multi-phase Flow in Power Engineering, Xi' an Jiaotong University, Xi' an, China, Post Code: 710049) // Journal of Engineering for Thermal Energy & Power. — 2007, 22(6). — 656 ~ 660

Through a three-dimensional numerical simulation, a study was conducted of the heat transfer and flow characteristics of restricted outgoing flows inside a spiral channel with different spiral angles (15°, 20°, 30°, 40°, 45°, 50°, 60°). The authors have proposed several optimization modes applicable in a certain range of Reynolds Number ($0.8\times10^4 \leqslant Re \leqslant 6\times10^4$), thereby improving the flow conditions and heat transfer at the shell side of a tube-and-shell type heat exchanger. The results of the study show that the restricted outgoing flow in the spiral channel can form an ideal plunger flow with the velocity distribution inside the channel being uniform, thus effectively minimizing and eliminating flow dead areas. Compared with a "Z"-shaped restricted outgoing flow formed by vertical baffles, the above-mentioned flow inside the spiral channel can boast a relatively high heat transfer coefficient and enjoy an obvious energy-saving effectiveness at a same pressure-drop gradient. In the range of Reynolds number under investigation, the flow in question has a comprehensive performance of optimum heat transfer and resistance when the spiral angle α is around 45°. The research findings can well provide a theoretical basis for the design of a high-efficiency and low-resistance structure at the shell side of a shell-and-tube type heat exchanger and for its further optimization. **Key words**: shell-and-tube type heat exchanger, restricted outgoing flow, spiral angle, numerical simulation, pressure drop

大型热力发电机组能耗参数的统计分析与应用＝**Statistical Analysis and Application of Energy-consumption Parameters of Large-sized Thermal Power Plants**[刊, 汉] / LI Li-ping, NIU Yu-guang (Automation College, North China Electric Power University, Baoding, China, Post Code: 071003), ZHANG Chun-fa, WANG Hui-jie (College of Energy Source and Power, North China Electric Power University, Baoding, China, Post Code: 071003) // Journal of Engineering for Thermal Energy & Power. — 2007, 22(6). — 661 ~ 664

Based on the long term operating data and on-line performance calculation ones of a power plant, a statistico-analytical study was performed of the actual performance characteristics of the plant. Proposed was a criterion for discriminating the plant performance steady state compatible with the process thermodynamic characteristics and thermal test standards. Through a statistical analysis of the sifted out data, which meet the steady-state criterion, obtained respectively was the un-

certainty range of the output of an on-line performance calculation model for plants under different outside boundary conditions, different operating parameters as well as identical operating conditions, thus providing useful reference data for optimization decision-making adjustment and diagnosis both based on the model in question. The coal consumption characteristic curves of the plant obtained through statistical calculations reflect the actual characteristics of the plant under real operating conditions. With the in-plant load distribution version serving as an example, the effectiveness of the measures taken for economic operation has been verified. **Key words**: thermal power plant, on-line performance calculation, statistical characteristics, uncertainty, load distribution

电站锅炉温室气体排放量的计算＝**Calculation of Greenhouse Gas Emissions from Utility Boilers**[刊, 汉] /LIU Huan-zhang, CHANG Tai-hua, LIU Ji-zhen, et al (Automation Department, North China Electric Power University, Beijing, China, Post Code: 102206)// Journal of Engineering for Thermal Energy & Power. — 2007, 22(6). —665 ~ 668

As an important secondary energy source, electric power is indispensable. However, a large quantity of waste emissions is produced during power generation, especially by coal-fired power plants. On the basis of flue gas analysis, a study of fuel characteristic coefficients and by analyzing combustion mechanism as well as through a modeling based on statistical laws, a forecast was given of the greenhouse gas carbon-dioxide emissions from coal-fired utility boilers. Finally, a simulation study was conducted of the forecasting method by making use of the real-time historic data from Panshan Power Plant. The simulation indicates the feasibility of the method under discussion. **Key words**: flue gas analysis, fuel characteristic coefficient, utility boiler, greenhouse gas

石灰石脱硫反应对喷氨脱硝反应影响的实验研究＝**An Experimental Study of the Effect of Limestone Desulfurization Reaction on Ammonia-injected Denitrification Reaction**[刊, 汉] /HOU Xiang-song, WANG Jin-wei, ZHANG Hai, et al (Education Ministry Key Laboratory on Thermal Science and Power Engineering, Thermal Energy Engineering Department, Tsinghua University, Beijing, China, Post Code: 100084)// Journal of Engineering for Thermal Energy & Power. — 2007, 22(6). —669 ~ 672

To inject ammonia into a CFB (circulating fluidized bed) boiler at its furnace tail portion or at the inlet of a cyclone separator can reduce the NO_x content in flue gases. In a CFB boiler, the injection of limestone for the purpose of desulfuration may influence the ammonia-injected denitrification reaction. An experimental study was conducted of the impact of pyrolytic and desulfuration products of the limestone on ammonia-injected denitrification reaction. It has been found that the pyrolytic reaction products of limestone prior to desulfuration have a relatively big specific surface area and CaO exhibits a definite catalytic activity, which can promote the ammonia-injected denitrification reaction. The desulfuration products of the limestone exercise a relatively small influence on the ammonia-injected denitrification reaction. When the temperature is above 1 200 K, however, the products in question can promote the oxidation of NH_3 and reduce the escape of NH_3, both aspects being considered as favorable to the ammonia-injected denitrification reaction. **Key words**: circulating fluidized bed, ammonia-sprayed denitrification, limestone, catalysis

喷淋脱硫塔喷嘴外流动数值模拟与实验研究＝**Numerical Simulation and Experimental Study of Flows Outside the Nozzles of a Spray-type Desulfuration Tower**[刊, 汉] /ZHOU Shan-ming, JIN Bao-sheng, SUN Zhi-ao (Education Ministry Key Laboratory on Clean Coal Power Generation and Combustion Technology, Southeast University, Nanjing, China, Post Code: 210096)// Journal of Engineering for Thermal Energy & Power. —2007, 22(6). —673 ~ 676

Established was a numerical simulation model for nozzles of a spray-type desulfuration tower and studied was the relationship among the following items, which can influence the gas-liquid mass transfer inside a spray type desulfuration tower: spray liquid flow rate, average rupture length of the liquid film, initial jet flow angle of the nozzle and average liquid drop diameter. A special test platform and single-turn spiral nozzle were designed and the liquid film and liquid-drop movement were tested and analyzed by using a quick-speed CCD (Charge Coupled Device) with a digital camera being used to take pictures. Both the model calculations and experimental results show that the average liquid film rupture-length and the average liquid drop diameter will decrease with an increase of spray liquid flow rate. When the clearance height at the nozzle